Applied Mathematical Modelling 37 (2013) 8629–8644

Contents lists available at SciVerse ScienceDirect

Applied Mathematical Modelling

journal homepage: www.elsevier.com/locate/apm

Analysis of vibration effects on the comfort of intercity bus users by oscillatory model with ten degrees of freedom

Dragan Sekulić [a], Vlastimir Dedović [a], Srdjan Rusov [a], Slaviša Šalinić [b,*], Aleksandar Obradović [c]

[a] University of Belgrade, Faculty of Transport and Traffic Engineering, Vojvode Stepe 305, 11000 Belgrade, Serbia
[b] University of Kragujevac, Faculty of Mechanical Engineering, Dositejeva 19, 36000 Kraljevo, Serbia
[c] University of Belgrade, Faculty of Mechanical Engineering, Kraljice Marije 16, 11120 Belgrade 35, Serbia

ARTICLE INFO

Article history:
Received 10 December 2011
Received in revised form 20 March 2013
Accepted 22 March 2013
Available online 16 April 2013

Keywords:
Comfort
ISO 2631
Road roughness
Simulation

ABSTRACT

The paper analyzes the effects of vibrations on the comfort of intercity bus IK-301 users. Evaluation of vibration effects was carried out according to the criteria set out in the 1997 ISO 2631-1 standard for comfort in public means of transport. Comfort is determined for the space of a driver, passenger in the middle part of the bus and passenger in the rear overhang. Also, the allowable exposure time to vibrations in drivers for the reduced comfort criterion was determined according to the 1978 ISO 2631-1 standard. The bus spatial oscillatory model with ten degrees of freedom was developed for the needs of the analysis. Bus excitation was generated applying the Power Spectral Density of the asphalt-concrete road roughness, as described by the H. Braun model. The allowable vibration exposure time for the driver's body decreases as the spring stiffness of the driver's seat suspension system increases. Simulation was performed using the MATLAB software.

1. Introduction

During the ride in a vehicle, drivers and passengers are exposed to vibrations from the road surface. Vibrations cause the feeling of discomfort, reduce working ability, and their lengthy action can affect health [1,2]. Drivers of construction machinery, farm machinery, heavy-duty vehicles and buses fall into a particularly risky group [3]. Investigations [3–5] have shown that bus drivers are exposed to high-intensity vibrations. The most common health problems in drivers due to long-term exposure to high-level vibrations are musculoskeletal disorders (low-back pain, neck, shoulders and kneel pains), mental disorders (tiredness, tension, mental fatigue), sleep disorder etc. [6,7]. In order to reduce adverse effects of vibrations and ensure health at workplaces, European Union adopted on 25 June 2002 the Directive 2002/44. It defines the allowable exposure limit values (thresholds) for whole-body vibrations at work and in accordance with those levels it is clearly emphasized that employers are obliged to ensure appropriate safety measures [8]. Timely action to prevent vibration injury in both drivers and passengers requires continuous monitoring of the vibration level they are exposed to. This means frequent measurements of the intensity of vibration exposure in users under real conditions of bus exploitation. Recently, the measurements of vibration levels in a vehicle in real conditions of its exploitation have been performed not only to analyse its oscillatory comfort, but also to assess the efficiency of the suspension system in the damping of vibrations transmitted from the vehicle wheels to its body. In [9] the signals of vertical accelerations were registered in the suspension system of a delivery car during its passing over a railway cross. The measurements of acceleration allowed for testing the suspension system quality in the damping of shock vibrations transmitted from the railway cross to the vehicle suspended mass. In [10] the analysis of

* Corresponding author. Tel./fax: +381 36 383269.
E-mail addresses: salinic.s@ptt.rs, salinic.s@mfkv.kg.ac.rs (S. Šalinić).

0307-904X/$ - see front matter © 2013 Elsevier Inc. All rights reserved.
http://dx.doi.org/10.1016/j.apm.2013.03.060

registered vertical acceleration signals in the vehicle suspension system, for three different types of excitations (asphalt, sett, and railway cross) has shown that the suspension system is more efficient in damping vibrations at higher frequency levels. Apart from measurements, analysis can be conducted by simulations using vehicle oscillatory model [11,12]. Simulations gain in importance in cases when measurements are seldom done due to various constraints. Quality analysis of the vehicle oscillatory behaviour requires integration of the previously recorded road roughness into the oscillatory model [12]. In this paper, because it was impossible to perform screening in real time of the road roughness, bus excitation was modelled using Power Spectral Density of the asphalt-concrete road roughness in a very good condition. The analysis of user's oscillatory comfort was carried out here by means of the spatial oscillatory model of the intercity bus IK-301 with ten degrees of freedom. The oscillatory comfort in the driver and passengers was assessed according to the procedure and criteria as prescribed by the 1997 ISO 2631-1 standard [13]. Also, it has been determined here the allowable vibration exposure time in drivers for the reduced comfort criterion, in accordance with the 1978 ISO 2631-1 standard [14].

2. Bus oscillatory model

The bus IK-301 (Fig. 1) has the suspension system with stiff axles [15]. Front axle (RABA/A 932.10) is attached to the body by means of two air bags and four telescopic shock absorbers, while rear axle (RABA/A 109.29) by means of four air bags and four telescopic shock absorbers. The bus has two wheels mounted on the front axle and four wheels on the rear axle. Fig. 2 shows the spatial oscillatory model of the bus IK-301 with ten degrees of freedom.

Independent motions of concentrated masses and stiff bodies of the considered mechanical oscillatory system are: vertical motions of the driver, the passenger in the middle part of the bus (passenger 1), the passenger in the bus rear overhang (passenger 2), the center of gravity of the bus mass-elastic system of suspension, and the centers of gravity of the front and rear axles, the angular motion of the bus mass-elastic system of suspension around the longitudinal and transverse axes (x-axis and y-axis) and angular motions of the bus front and rear axles around the axes x_1 and x_2. Fig. 3 gives a schematic representation of the elements of suspension on the rear axle with characteristic geometry which has been used to determine the corresponding stiffness and damping for the oscillatory model depicted in Fig. 2.

Effects of vibrations transmitted from the road to the bodies of the driver and passengers also depend on the properties of the seat suspension system. Driver's seat is equipped with the pneumatic elastic suspension and a shock absorber. Passengers' seats are stiff-suspended, and seats' air bags are of hard polyurethane foam [15]. Elastic-damping properties of these seats are presented in Table 3. Positions of driver's seat, of passengers' in the middle part of the bus and of those in the rear overhang are indicated by numbers 1, 2 and 3, respectively, in Fig. 4. Also, in Fig. 4 the position of the center of gravity of a fully loaded bus is denoted.

The adopted assumptions for the bus oscillatory model are as follows:

- the bus is symmetrical relative to the longitudinal center of gravity axis (x-axis);
- all possible motions of concentrated masses around the position of stationary equilibrium are small;
- the bus body, front and rear axles are rigid bodies;
- the bus engine is included in the bus body, so that engine oscillatory excitation has not been taken into account;
- characteristics of all elastic and damping elements are linear;
- bus wheels are in permanent contact with the road surface;
- the bus is moving along a straight line with constant speed.

The properties of the spring and shock-absorber in the vehicle suspension system as well as those of the tyres and other vehicle elastic elements are nonlinear. Therefore, vehicle nonlinear oscillatory models are used in oscillatory behaviour analyses [16]. In [17] a plane nonlinear oscillatory model with 4DOF is presented, while in [18] a spatial nonlinear oscillatory model with 7DOF to study the vehicle chaotic response.

The notations in Figs. 2–4 are interpreted in Tables 1–3. All values of parameters, originating from literature available [15,19–21], used in the simulation are also given in Tables 1–3.

Fig. 1. Intercity bus IK-301.

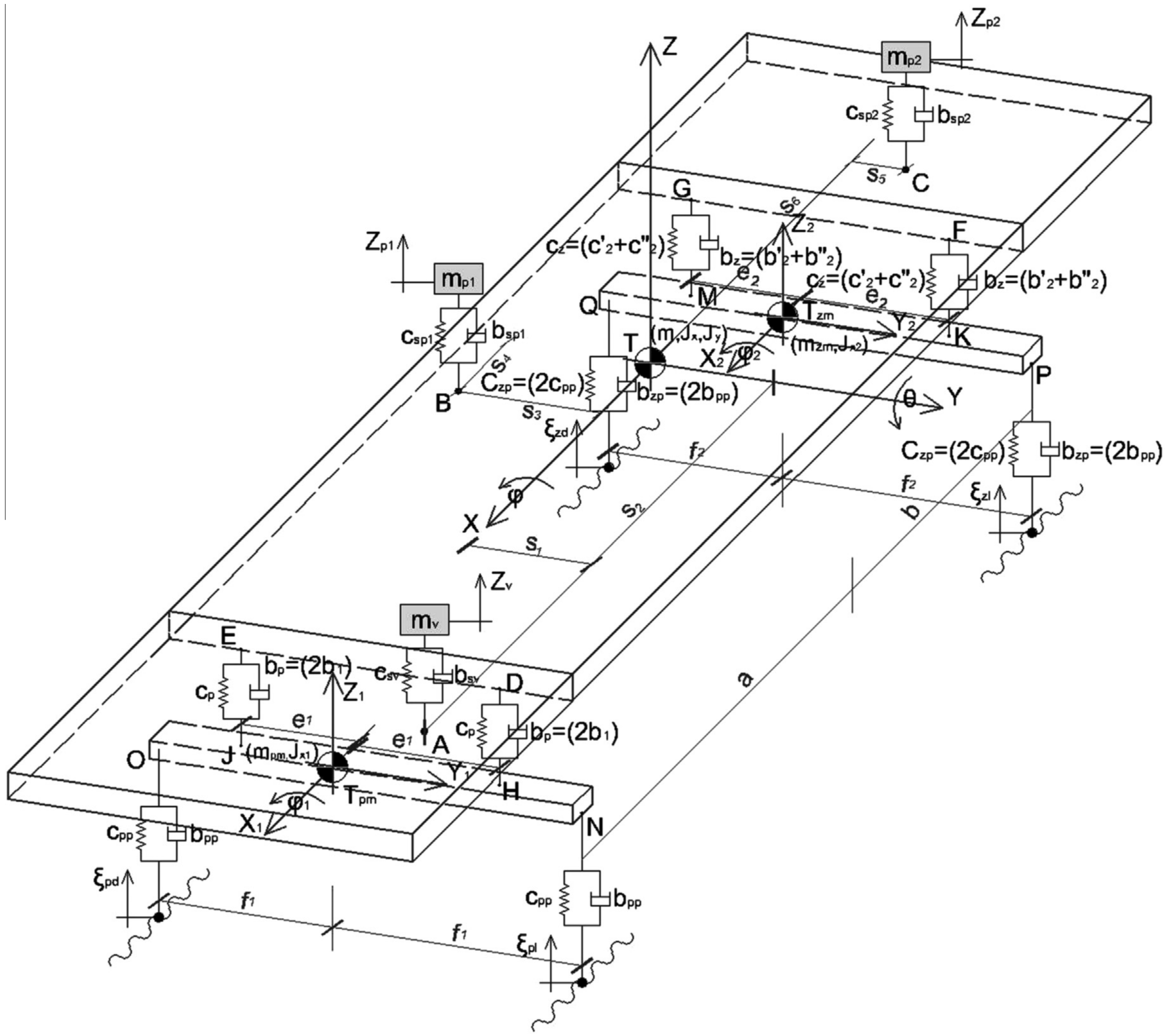

Fig. 2. Oscillatory model of the bus IK-301.

According to Fig. 3, the equivalent stiffness and damping values are calculated using the following expressions:

$$c_z = c_2' + c_2'' = \frac{c_2(b - r_a)^2}{b^2} + \frac{c_2(b + r_a)^2}{b^2}, \tag{1}$$

$$b_z = b_2' + b_2'' = \frac{b_2(b - r_a)^2}{b^2} + \frac{b_2(b + r_a)^2}{b^2}. \tag{2}$$

The analysis of the oscillatory comfort for the bus driver and passengers requires the determination of differential equations of motion corresponding to the oscillatory model shown in Fig. 2. Applying Lagrange's equations of the second kind and taking into account the above assumptions, the differential equations of motion are obtained as follows:

$$m_v\ddot{z}_v + b_{sv}\dot{z}_v + c_{sv}z_v - b_{sv}\dot{z} - c_{sv}z - s_1 b_{sv}\dot{\varphi} - s_1 c_{sv}\varphi + s_2 b_{sv}\dot{\theta} + s_2 c_{sv}\theta = 0, \tag{3}$$

$$m_{p1}\ddot{z}_{p1} + b_{sp1}\dot{z}_{p1} + c_{sp1}z_{p1} - b_{sp1}\dot{z} - c_{sp1}z + s_3 b_{sp1}\dot{\varphi} + s_3 c_{sp1}\varphi + s_4 b_{sp1}\dot{\theta} + s_4 c_{sp1}\theta = 0, \tag{4}$$

$$m_{p2}\ddot{z}_{p2} + b_{sp2}\dot{z}_{p2} + c_{sp2}z_{p2} - b_{sp2}\dot{z} - c_{sp2}z - s_5 b_{sp2}\dot{\varphi} - s_5 c_{sp2}\varphi - s_6 b_{sp2}\dot{\theta} - s_6 c_{p2}\theta = 0, \tag{5}$$

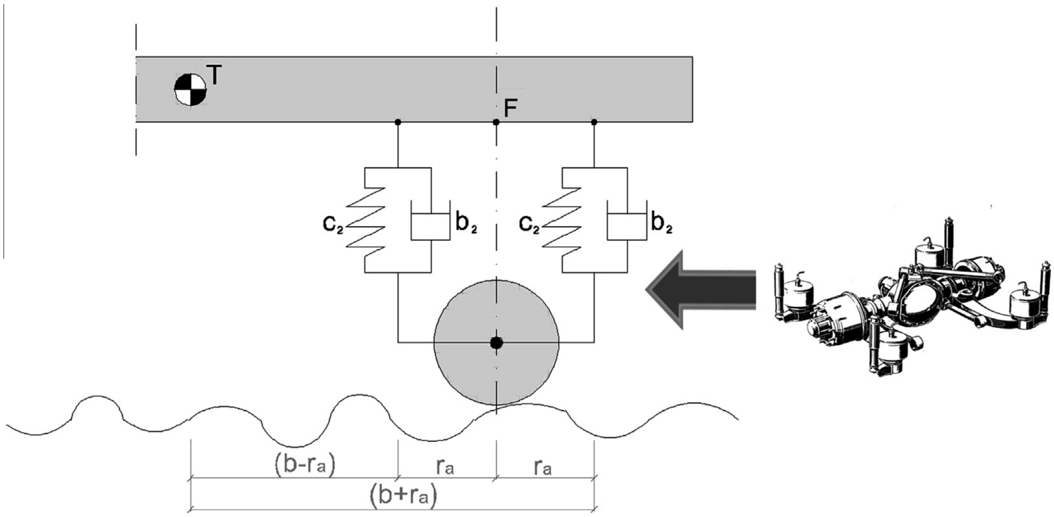

Fig. 3. Elements of suspension on the bus IK-301 rear axle.

Table 1
Geometric parameters of the bus IK-301.

Geometric parameters	Description	Values
l	Wheelbase	5.65 m
a	Distance from the front axle to the bus center of gravity	3.61 m
b	Distance from the rear axle to the bus center of gravity	2.04 m
f_1	Distance from the front right and left wheel to the front axle center of gravity	1.00 m
e_1	Distance from suspension elements on the front axle to the front axle center of gravity and longitudinal x-axis, respectively	0.70 m
f_2	Distance from the rear right and left wheel to the rear axle center of gravity	1.00 m
e_2	Distance from suspension elements on the rear axle to the rear axle center of gravity and longitudinal x-axis, respectively	0.80 m
s_1	Distance from the driver seat to longitudinal x-axis	0.65 m
s_2	Distance from the driver seat to transverse y-axis	5.45 m
s_3	Distance from the passenger 1 seat to longitudinal x-axis	0.80 m
s_4	Distance from the passenger 1 seat to transverse y-axis	0.50 m
s_5	Distance from the passenger 2 seat to longitudinal x-axis	0.40 m
s_6	Distance from the passenger 2 seat to transverse y-axis	4.20 m
r_a	Distance from the rear axle suspension elements to the rear axle	0.30 m

Table 2
Mass parameters of the bus IK-301.

Mass parameters	Description	Values
m_v	Mass of the driver and seat	100 kg
m_{p1}	Mass of the passenger 1 and seat	90 kg
m_{p2}	Mass of the passenger 2 and seat	90 kg
m	elastic-suspended mass of the fully loaded bus	15,890 kg
m_{pm}	The front axle mass	746 kg
m_{zm}	The rear axle mass	1355 kg
J_x	The suspended mass moment of inertia relative to the x-axis	13,000 kg m^2
J_y	The suspended mass moment of inertia relative to the -yaxis	150,000 kg m^2
J_{x1}	The front axle moment of inertia relative to the x_1 axis	350 kg m^2
J_{x2}	The rear axle moment of inertia relative to the x_2 axis	620 kg m^2

$$m\ddot{z} + (b_{sv} + b_{sp1} + b_{sp2} + 2b_p + 2b_z)\dot{z} + (c_{sv} + c_{sp1} + c_{sp2} + 2c_p + 2c_z)z + (s_1 b_{sv} - s_3 b_{sp1} + s_5 b_{sp2})\dot{\varphi} + (s_1 c_{sv} - s_3 c_{sp1} + s_5 c_{sp2})\varphi - (s_2 b_{sv} + s_4 b_{sp1} - s_6 b_{sp2} + 2ab_p - 2bb_z)\dot{\theta} - (s_2 c_{sv} + s_4 c_{sp1} - s_6 c_{sp2} + 2ac_p - 2bc_z)\theta - b_{sv}\dot{z}_v - c_{sv}z_v - b_{sp1}\dot{z}_{p1} - c_{sp1}z_{p1} - b_{sp2}\dot{z}_{p2} - c_{sp2}z_{p2} - 2b_p\dot{z}_1 - 2c_p z_1 - 2b_z\dot{z}_2 - 2c_z z_2 = 0, \tag{6}$$

Table 3
Oscillatory parameters of the bus IK-301.

Oscillatory parameters	Description	Values
c_{sv}	Spring stiffness of the driver seat suspension system	10,000 N/m
b_{sv}	Shock-absorber damping of the driver seat suspension system	750 Ns/m
c_{sp1}, c_{sp2}	Seat stiffness of the passenger 1 and passenger 2 seats	40,000 N/m
b_{sp1}, b_{sp2}	Damping of the passenger 1 and passenger 2 seats	220 Ns/m
c_p	Single air bag stiffness on the front axle	175,000 N/m
b_1	Single shock-absorber stiffness on the front axle	20,000 Ns/m
b_p	Equivalent shock-absorber damping on the left and the right side of the front axle	40,000 Ns/m
c_2	Single air bag stiffness on the rear axle	200,000 N/m
c_z	Equivalent air bags stiffness on the left and the right side of the rear axle	408,650 N/m
b_2	Single shock-absorber damping on the rear axle	22,500 Ns/m
b_z	Equivalent shock-absorber damping on the left and the right side of the rear axle	45,973 Ns/m
c_{pp}	Single tyre stiffness on the front and the rear axle	1,000,000 N/m
c_{zp}	Equivalent tyre stiffness on the left and the right side of the rear axle	2,000,000 N/m
b_{pp}	Single tyre damping on the front and the rear axle	150 Ns/m
b_{zp}	Equivalent tyre damping on the left and the right side of the rear axle	300 Ns/m

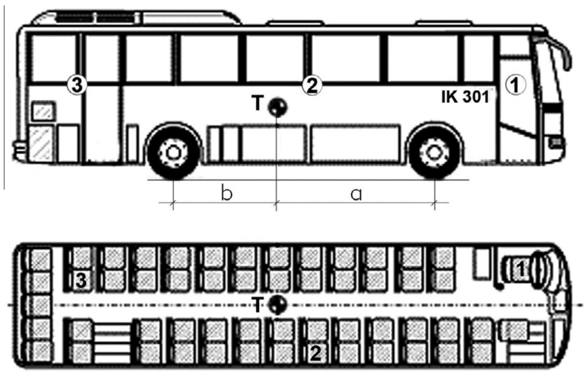

Fig. 4. Bus driver and passengers' seats and position of the bus center of gravity.

$$\begin{aligned}
&J_x\ddot{\varphi} + \left(s_1^2 b_{sv} + s_3^2 b_{sp1} + s_5^2 b_{sp2} + 2e_1^2 b_p + 2e_2^2 b_z\right)\dot{\varphi} + \left(s_1^2 c_{sv} + s_3^2 c_{sp1} + s_5^2 c_{sp2} + 2e_1^2 c_p + 2e_2^2 c_z\right)\varphi - s_1 b_{sv}\dot{z}_v \\
&\quad - s_1 c_{sv} z_v + s_3 b_{sp1}\dot{z}_{p1} + s_3 c_{sp1} z_{p1} - s_5 b_{sp2}\dot{z}_{p2} - s_5 c_{sp2} z_{p2} + \left(s_1 b_{sv} - s_3 b_{sp1} + s_5 b_{sp2}\right)\dot{z} + \left(s_1 c_{sv} - s_3 c_{sp1} + s_5 c_{sp2}\right) z \\
&\quad - \left(s_1 s_2 b_{sv} - s_3 s_4 b_{sp1} - s_5 s_6 b_{sp2}\right)\dot{\theta} - \left(s_1 s_2 c_{sv} - s_3 s_4 c_{sp1} - s_5 s_6 c_{sp2}\right)\theta - 2e_1^2 b_p\dot{\varphi}_1 - 2e_1^2 c_p\varphi_1 - 2e_2^2 b_z\dot{\varphi}_2 - 2e_2^2 c_z\varphi_2 = 0,
\end{aligned} \tag{7}$$

$$\begin{aligned}
&J_y\ddot{\theta} + \left(s_2^2 b_{sv} + s_4^2 b_{sp1} + s_6^2 b_{sp2} + 2a^2 b_p + 2b^2 b_z\right)\dot{\theta} + \left(s_2^2 c_{sv} + s_4^2 c_{sp1} + s_6^2 c_{sp2} + 2a^2 c_p + 2b^2 c_z\right)\theta \\
&\quad + s_2 b_{sv}\dot{z}_v + s_2 c_{sv} z_v + s_4 b_{sp1}\dot{z}_{p1} + s_4 c_{sp1} z_{p1} - s_6 b_{sp2}\dot{z}_{p2} - s_6 c_{sp2} z_{p2} - \left(s_2 b_{sv} + s_4 b_{sp1} - s_6 b_{sp2} + 2ab_p - 2bb_z\right)\dot{z} \\
&\quad - \left(s_2 c_{sv} + s_4 c_{sp1} - s_6 c_{sp2} + 2ac_p - 2bc_z\right) z - \left(s_1 s_2 b_{sv} - s_3 s_4 b_{sp1} - s_5 s_6 b_{sp2}\right)\dot{\varphi} - \left(s_1 s_2 c_{sv} - s_3 s_4 c_{sp1} - s_5 s_6 c_{sp2}\right)\varphi \\
&\quad + 2ab_p\dot{z}_1 + 2ac_p z_1 - 2bb_z\dot{z}_2 - 2bc_z z_2 = 0,
\end{aligned} \tag{8}$$

$$m_{pm}\ddot{z}_1 + 2(b_p + b_{pp})\dot{z}_1 + 2(c_p + c_{pp})z_1 - 2b_p\dot{z} - 2c_p z + 2ab_p\dot{\theta} + 2ac_p\theta = b_{pp}\dot{\xi}_{pd} + c_{pp}\xi_{pd} + b_{pp}\dot{\xi}_{pl} + c_{pp}\xi_{pl}, \tag{9}$$

$$J_{x1}\ddot{\varphi}_1 + 2\left(e_1^2 b_p + f_1^2 b_{pp}\right)\dot{\varphi}_1 + 2\left(e_1^2 c_p + f_1^2 c_{pp}\right)\varphi_1 - 2e_1^2 b_p\dot{\varphi} - 2e_1^2 c_p\varphi = -f_1 b_{pp}\dot{\xi}_{pd} - f_1 c_{pp}\xi_{pd} + f_1 b_{pp}\dot{\xi}_{pl} + f_1 c_{pp}\xi_{pl}, \tag{10}$$

$$m_{zm}\ddot{z}_2 + 2(b_z + b_{zp})\dot{z}_2 + 2(c_z + c_{zp})z_2 - 2b_z\dot{z} - 2c_z z - 2bb_z\dot{\theta} - 2bc_z\theta = b_{zp}\dot{\xi}_{zd} + c_{zp}\xi_{zd} + b_{zp}\dot{\xi}_{zl} + c_{zp}\xi_{zl}, \tag{11}$$

$$J_{x2}\ddot{\varphi}_2 + 2\left(e_2^2 b_z + f_2^2 b_{zp}\right)\dot{\varphi}_2 + 2\left(e_2^2 c_z + f_2^2 c_{zp}\right)\varphi_2 - 2e_2^2 b_z\dot{\varphi} - 2e_2^2 c_z\varphi = -f_2 b_{zp}\dot{\xi}_{zd} - f_2 c_{zp}\xi_{zd} + f_2 b_{zp}\dot{\xi}_{zl} + f_2 c_{zp}\xi_{zl}. \tag{12}$$

Oscillatory vertical excitations (road roughness) of the mechanical oscillatory system are introduced in the contact of the bus front and rear wheel tyres with the road surface. In differential equations (9) and (10) there figure road roughness on the bus front right and the front left wheels, ξ_{pd} and ξ_{pl}, respectively. Road roughness on the rear right and the rear left wheels, ξ_{zd} and ξ_{zl}, respectively, figure in differential Eqs. (11) and (12) and they are described as

$$\xi_{zd}(t) = \xi_{pd}(t - t_1) = \xi_{pd}\left(t - \frac{l}{V}\right),$$

$$\xi_{zl}(t) = \xi_{pl}(t - t_1) = \xi_{pl}\left(t - \frac{l}{V}\right), \tag{13}$$

where t_1 is time delay of the bus rear wheels in s, l is bus wheelbase in m, and V is bus speed in m/s.

A software for numerical solving of the differential equations was written in the MATLAB program package, where the MATLAB built-in Runge–Kutta routine "*ode*45()" with a variable step-size of numerical integration was used. The defined initial conditions for all variables are equal to zero. The chosen simulation time is 7 s.

3. Bus excitation

The longitudinal road roughness is of a stochastic nature and can be represented as a stationary and ergodic random process. Measurements indicated that the road roughness is subject to the normal (Gaussian) distribution. The longitudinal road roughness can be described not only by stochastic quantities, but also in a frequency domain by means of the Power Spectral Density (PSD) of the road roughness. The PSD has been defined by a number of authors. The H. Braun model has been accepted as a basis for a number of standards in this field [2]. The Braun stochastic model is used to describe the excitation at a single point on a single track as follows:

$$\Phi_\xi(v) = \Phi_\xi(v_0)\left(\frac{v}{v_0}\right)^{-w} \tag{14}$$

where v is the spatial frequency in m^{-1}, v_0 is the reference spatial frequency in m^{-1}, $\Phi_\xi(v_0)$ is the road roughness coefficient corresponding to the value v_0 expressed in m^3, and w is the exponent of the fitted PSD. In this paper the asphalt-concrete road roughness in a very good condition has been modelled for the bus excitation. Table 4 gives characteristic values of coefficients for this type and condition of the road for $v_0 = 1$ m^{-1}.

For the road roughness modelling in a time domain, it is suitable to express the PSD of the road roughness as a function of the temporal frequency of excitation. The relationship between the power spectral densities expressed as a function of the temporal frequency of excitation and the spatial frequency is given by

$$\Phi_\xi(\Omega) = \frac{1}{V}\Phi_\xi(v) \tag{15}$$

where Ω is the temporal frequency of excitation in Hz, and V is the constant speed of the vehicle in m/s. Based on the relationship between the temporal and spatial frequencies

$$\Omega = vV \tag{16}$$

the Braun stochastic model can be represented in the following form:

$$\Phi_\xi(\Omega) = V^{w-1}\Phi_\xi(v_0)\left(\frac{v_0}{\Omega}\right)^{w} \tag{17}$$

Fig. 5 shows the dependence of the PSD of the road roughness on the temporal frequency of excitation for the vehicle speed of 100 km/h and the coefficient values given in Table 4. As the road roughness in the frequency range 0.5 Hz—50 Hz is of particular importance for the oscillatory comfort analysis [22], the PSD of the road roughness is shown in Fig. 5 for the mentioned range.

3.1. Generation of the road longitudinal roughness

The road roughness has been obtained here by the model for the random process simulation used by Shinozuka [23]. A random process, according to [23], can be represented by an infinite sum of harmonic cosine functions of different amplitudes, circular frequencies and phase angles. Using this model, the single-track road roughness can be described by the following analytical expression:

$$\xi(t) = \sum_{i=1}^{N} A_i \cos(2\pi\Omega_i t + \alpha_i) \tag{18}$$

Table 4
Frequency spectrum mean value of the asphalt-concrete road for $v_0 = 1(\mathrm{m}^{-1})$.

Type of road surface	Condition (subjective)	Mean value	
		w	Coefficient of road roughness $\Phi_\xi(v_0)$
Asphalt concrete	Very good	2.2	1.3

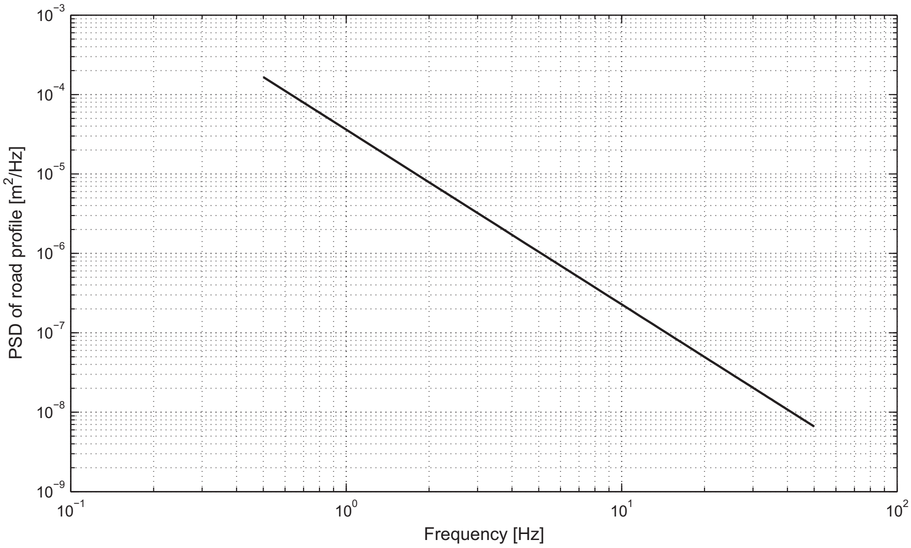

Fig. 5. PSD of the asphalt-concrete road roughness in a very good condition as a function of the temporal frequency for the vehicle speed of 100 km/h.

where N is the number of harmonics, α_i is the independent random phase angles uniformly distributed in the interval $[0, 2\pi]$, Ω_i is the discrete frequencies of excitation in Hz, and A_i is the discrete amplitudes of excitation expressed in m. The frequencies Ω_i are calculated according to

$$\Omega_i = \Omega_l + \left(i - \frac{1}{2}\right)\Delta\Omega \tag{19}$$

where $\Delta\Omega$ is a frequency step that can be represented by the expression

$$\Delta\Omega = \frac{\Omega_u - \Omega_l}{N} \tag{20}$$

and where $\Omega_l = 0.5$ Hz and $\Omega_u = 50$ Hz are the lower and upper bounds of the considered excitation frequency interval, respectively. Also, the discrete amplitudes of excitation A_i can be calculated by the expression

$$A_i = \sqrt{2\Phi_\xi(\Omega_i)\Delta\Omega}. \tag{21}$$

Note that when $N \to \infty$, applying the central limit theorem, it can be shown, based on (19) and (21), that the road roughness $\xi(t)$ tends to the ergodic Gaussian stationary process, while the PSD of the road roughness $\xi(t)$ tends to $\Phi_\xi(\Omega)$.

Road longitudinal roughness, in good and bad condition according to ISO 8608, modelled by means of (18), was used in [24] for excitation of quarter-car models with 2DOF: linear model, nonlinear model with bilinear suspension damper and nonlinear model with the "sky-hook" characteristic. Besides the roughness signal obtained using (18), other signals of the road modelled roughness are in use for oscillatory excitations. In [25] signals of white and coloured noise respectively are used for excitations of nonlinear quarter-car models with 1DOF and 2DOF. In [26] for the excitation of nonlinear quarter-car model with 1DOF, a combination of the harmonic function and noise has been taken as follows:

$$x_0(t) = A\sin(2\pi V_0 t/\lambda) + \psi(V_0 t) \tag{22}$$

where A is harmonic excitation amplitude in m, λ is roughness wavelength in m, V_0 is vehicle speed in m/s, and $\psi(V_0 t)$ is excitation stochastic component in m, modelled as white noise in [26]

Further, if it is assumed that the left-track road roughness has been described by the expression (18) and that there is a correlation between the left and right-track roughnesses, then the vehicle right-track excitation can be obtained by the cross-spectral density function. Another track excitation (e.g. right), based on [27], can be represented by

$$\xi_d(t) = \sum_{i=1}^{N}\left[\sqrt{2\Phi_{\xi_l\xi_d}(\Omega_i)\Delta\Omega}\cos(2\pi\Omega_i t + \alpha_i) + \sqrt{2\left(\Phi_\xi(\Omega_i) - \Phi_{\xi_l\xi_d}(\Omega_i)\right)\Delta\Omega}\cos(2\pi\Omega_i t + \beta_i)\right] \tag{23}$$

where β_i is the independent random phase angles uniformly distributed in the interval $[0, 2\pi]$ and $\Phi_{\xi_l\xi_d}(\Omega_i)$ is the cross-spectral density function in m^2/Hz given by

$$\Phi_{\xi_l\xi_d}(\Omega_i) = \gamma_i\Phi_\xi(\Omega_i). \tag{24}$$

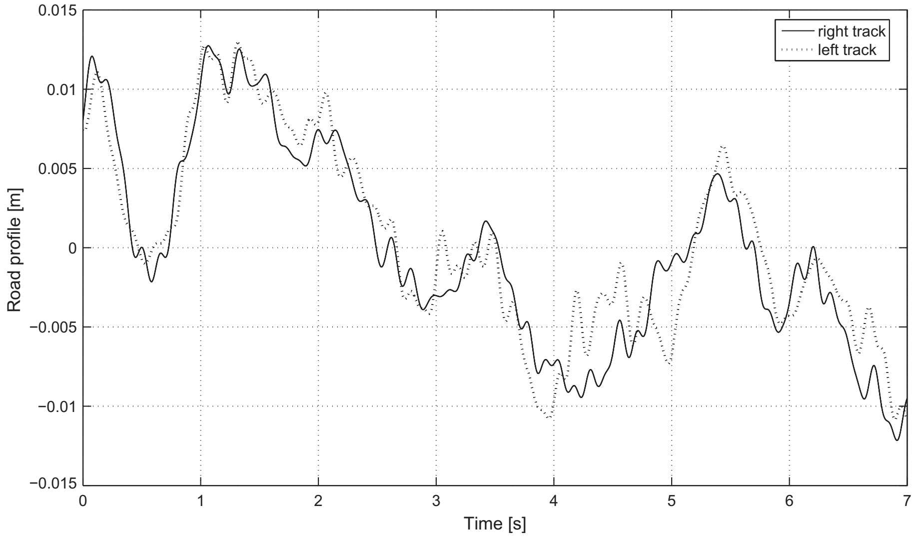

Fig. 6. Generated asphalt-concrete road roughness (very good) as a function of time for bus speed of 100 km/h.

In (24), γ_i is the square of transfer function filter module for discrete frequencies of excitation defined by

$$\gamma_i = \frac{v_l^2}{v_l^2 + \left(\frac{\Omega_i}{V}\right)^2} \tag{25}$$

where v_l is the cut-off frequency whose value was found by measurements and amounts to 0.2 m^{-1} (see [27]).

In accordance to the above relations, the procedure for generating the road roughness of a specified type and condition can be described by the following steps:

1. to define power spectral density for a particular speed of the vehicle according to (17);
2. to generate $p_{i(i=1-N)}$ realizations of the random variable $p \sim U(0,1)$;
3. to generate $n_{i(i=1-N)}$ realizations of the random variable $n \sim U(0,1)$;
4. to calculate the values $\alpha_i(\alpha_i = 2\pi p_i)$ and $\beta_i(\beta_i = 2\pi n_i)$ of random variables α and β, so that mentioned variables have the uniform distribution in the interval $[0, 2\pi]$, i.e., $\alpha \sim U(0, 2\pi)$ and $\beta \sim U(0, 2\pi)$;
5. to define the lower and upper bounds of the excitation frequency interval (values Ω_l and Ω_u);
6. to define the number of harmonics N and the frequency step $\triangle\Omega$;
7. to determine the single track (e.g. left) road roughness according to the expression (18);
8. to calculate the cross-spectral density function according to the expression (24);
9. to determine the another track (e.g. right) road roughness according to the expression (23).

Based on the above given procedure, using the Matlab software, simulations were carried out for the type and condition of the road surface from Table 4 and for the bus speed of 100 km/h. Realizations of random variables $p \sim U(0,1)$ and $n \sim U(0,1)$ were obtained by using the MATLAB built-in function "(*rand*)" (see [28]). The right and the left-track roughness was determined each for $N = 1000$ harmonics.

Fig. 6 shows the generated asphalt-concrete road roughness in a very good condition as a function of time for the bus speed of 100 km/h.

4. Analysis of simulation results

Assessment of vibration effects on the comfort of bus users was carried out by the procedure as regulated by the international 1997 ISO 2631-1 standard [13]. It prescribes the vibration total value of weighted root mean square accelerations as a reference quantity for the assessment of vibration effects on the comfort. In this paper, the analysis of comfort was carried out relative to the calculated root mean square of the weighted acceleration for the vertical direction on the places of the driver and passengers, that is,

$$\ddot{z}_{rms,w} = \sqrt{\frac{1}{T}\int_0^T \ddot{z}_w^2(t)dt} \tag{26}$$

where $\ddot{z}_{rms,w}$ is the root mean square of the weighted acceleration for the vertical direction expressed in m/s^2, $\ddot{z}_w(t)$ is the weighted acceleration amplitude for the vertical direction expressed in m/s^2, and T is the time exposure duration in s. The weighted acceleration $\ddot{z}_w(t)$ was obtained by filtering the signals of vertical acceleration on users' places $\ddot{z}(t)$ through the frequency-weighting curve W_k defined in the 1997 ISO 2631-1 standard for the comfort analysis of human whole-body exposure to oscillations at a sitting position. The weighting filter, in essence, reflects the human body sensitivity to vibrations, depending on frequencies. The human body is most sensitive to the vertical acceleration in the frequency range of 4 Hz $\div$ 8 Hz. Outside this range, susceptibility decreases with the frequency decrease below 4 Hz and with the frequency increase above 8 Hz. Consequently, the transfer function filter module W_k for frequencies in the range 4 Hz—8 Hz is equal to unity. In the MATLAB software the frequency-weighting curve W_k (Fig. 7) was defined in accordance with the 1997 ISO 2631-1 standard, which was used to obtain the weighted acceleration for the bus users. For the analog–digital transformation of the transfer functions of the band-pass and weighting filters, the MATLAB built-in routine "*bilinear*()" was employed.

The assessment of comfort was carried out by comparing the simulation-established root mean squares of the weighted acceleration on the bus users (Table 5), as defined by the 1997 ISO 2631-1 standard (see Fig. 8).

For the excitation of asphalt-concrete in a very good condition, vibrations do not produce any effects on the comfort of driver and passenger 1. The root mean square of the weighted acceleration for passenger 2 for the bus speed of 100 km/h amounts to 0.62 m/s^2. According to the weighting criteria, as prescribed by the 1997 ISO 2631-1 standard, vibrations have effects on the comfort of passenger 2, denoted as "rather uncomfortable".

4.1. Analysis of seat oscillatory parameters effects on driver comfort

Vibrations are transmitted from the bus floor via the driver seat suspension system to the driver's body. The basic elements of the driver seat suspension system are an air spring (pneumatic balloon) and a hydraulic shock-absorber. Effects of vibrations on the bus driver oscillatory comfort depend on the spring stiffness and the shock-absorber damping. Figs. 9–11 show changes in the driver's vertical acceleration for various values of the spring stiffness ($c_{sv} = 5000, 10,000$, and $15,000$ N/m) and various values of the shock-absorber damping ($b_{sv} = 400, 750$, and 1000 N/m) of the driver's seat.

It is noticeable that as the spring stiffness increases by a single constant value of the shock-absorber damping, the values of the driver's vertical acceleration increase as well. Fig. 12 shows the vertical acceleration signal on the driver's place of the intercity bus IK-302 obtained by measurements in prior researches [20].

The signal was recorded at constant speed of bus motion at 100 km/h on the section of the "Aerodrom – Ikarbus" road with the asphalt-concrete roadway in a very good condition. Three-axis accelerator B&K, type B&K 4321 was used for signal recording, while an amplifier of the B&K type was employed for amplifying the output signal from the accelerator (Fig. 12). The amplification on the amplifier was chosen so that the acceleration of 10 m/s^2 corresponds to the voltage of 1 V. Fig. 13 shows a parallel representation of vertical acceleration signals on a bus driver's seat established by experimental measurements (black line) and simulation (red line). The measured peak values of the vertical acceleration are 1.5 m/s^2 and -1.2 m/s^2, while almost all values for the vertical acceleration signal are in the range of -0.6 m/s^2 $\div$ 0.6 m/s^2 (see Fig. 13). The peak values of the driver's vertical acceleration established by simulation for driver seat real oscillatory parameters ($c_{sv} = 10,000$ N/m, $b_{sv} = 750$ Ns/m) are 1.3 m/s^2 and -1.4 m/s^2 (see Fig. 13). For a larger part of simulation time the

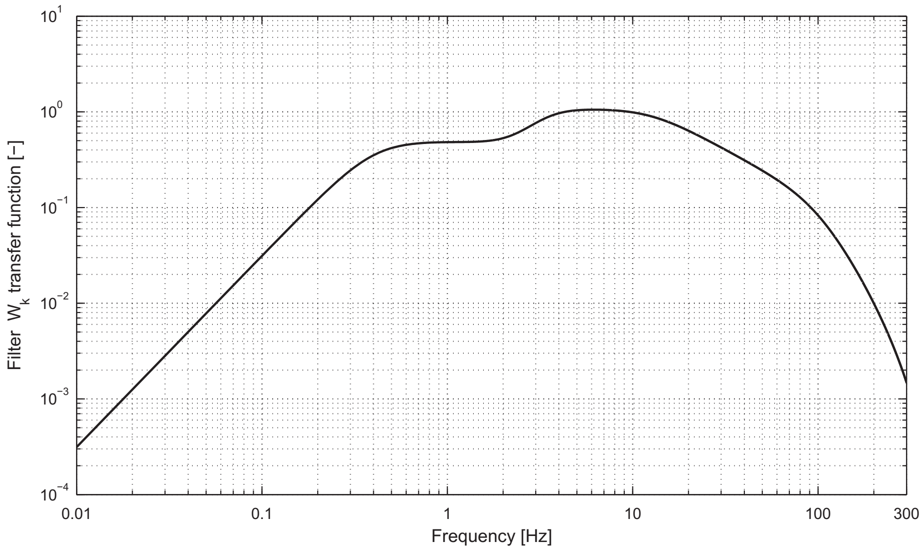

Fig. 7. Weighting filter W_k for vertical acceleration on users, after 1997 ISO 2631-1.

Table 5
Root mean squares of the weighted acceleration on the bus users.

Type and condition of the road	Bus speed (km/h)	Root mean square of the weighted acceleration (m/s^2)		
		Driver	Passenger1	Passenger2
Asphalt-concrete (very good)	100	0.23	0.30	0.62

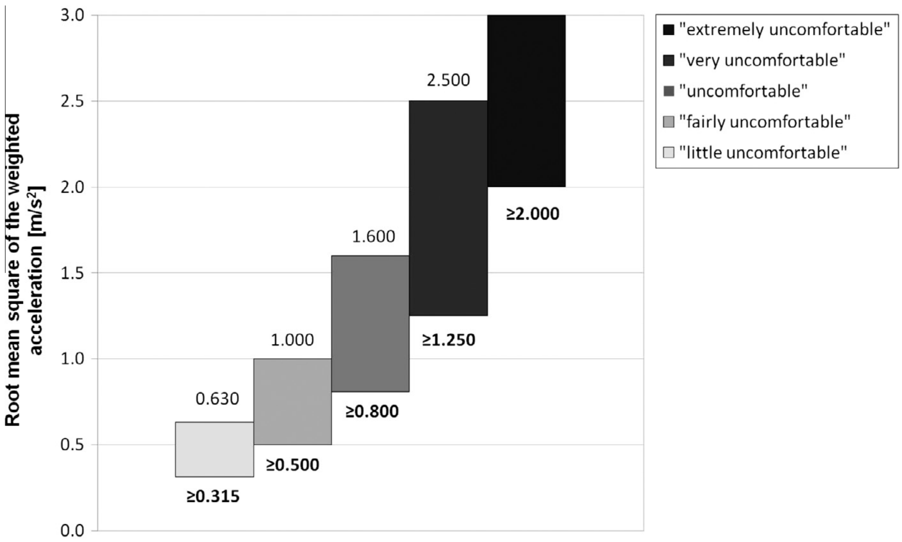

Fig. 8. Criteria for comfort in public means of transport depending on root mean square of the weighted acceleration, after 1997 ISO 2631-1.

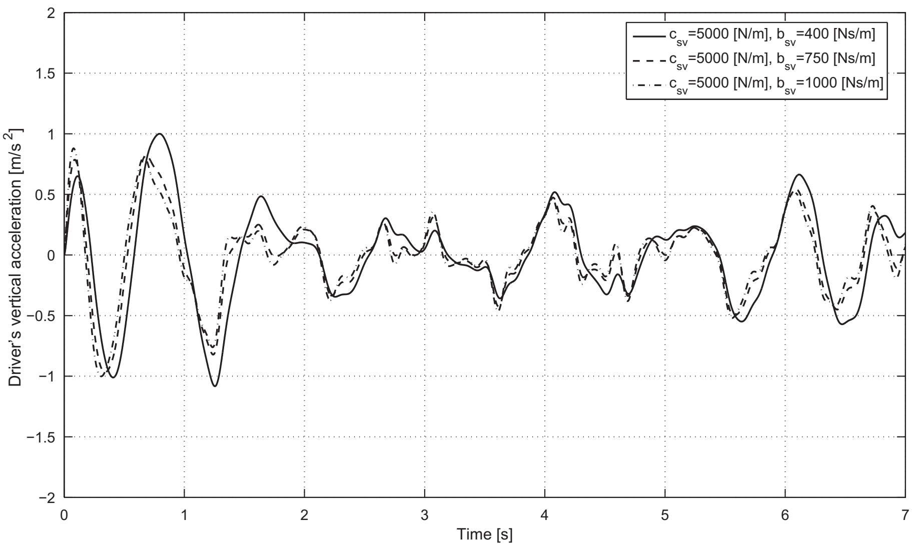

Fig. 9. Driver's vertical acceleration for the spring stiffness of 5000 N/m and various values of the shock-absorber damping.

values of the driver's vertical acceleration are in the range of $-0.5\ m/s^2 \div 0.5\ m/s^2$ with a similar nature of change like a real acceleration signal.

Table 6 shows statistical values for the drives vertical acceleration established by measurements and simulation. The measured driver's acceleration mean value equals zero, while acceleration mean value established by simulation approximates zero and amounts to $-0.0006\ m/s^2$. Also, acceleration dispersions differ slightly (0.40 for measurements and 0.2228 for simulation). Consequently, the bus oscillatory model allows for a good assessment of the driver's vertical acceleration signal.

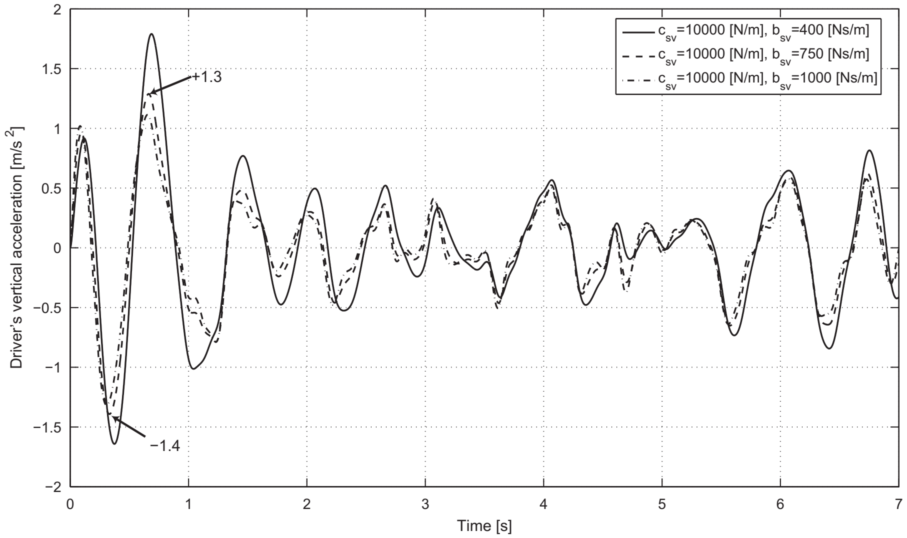

Fig. 10. Driver's vertical acceleration for the spring stiffness of 10,000 N/m and various values of the shock-absorber damping.

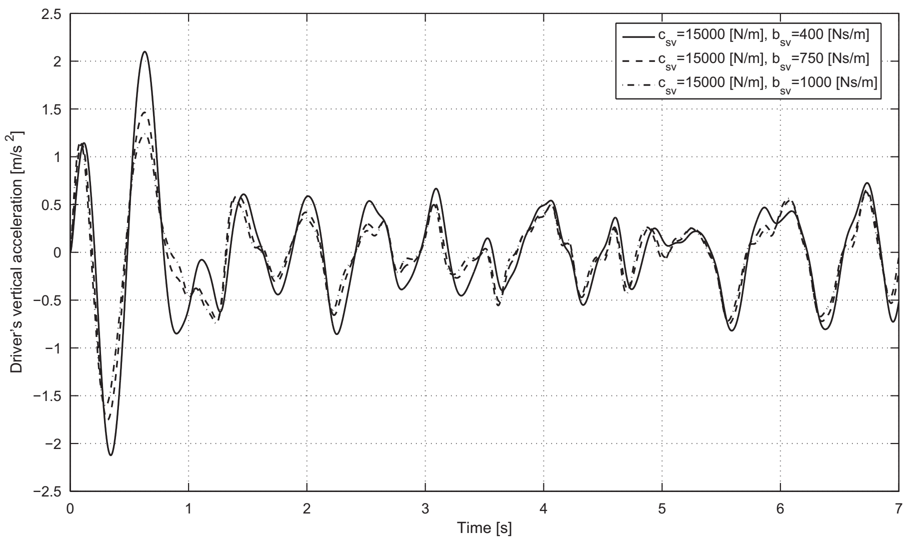

Fig. 11. Driver's vertical acceleration for the spring stiffness of 15,000 N/m and various values of shock-absorber damping.

It should be pointed out that, based on the simulation results, values of the driver's vertical acceleration signal can be reduced with low stiffness springs. Indeed, for the spring stiffness of 5000 N/m and the shock-absorber damping of 750 Ns/m, the peak values for the driver's vertical acceleration are in the range of $-1\ \mathrm{m/s^2} \div 1\ \mathrm{m/s^2}$ (see Fig. 9). Table 7 gives root mean squares of the weighted driver's acceleration for the spring stiffnesses of 5000, 10,000, and 15,000 N/m and the values of the shock-absorber damping coefficients for the driver's seat of 400, 750, and 1000 Ns/m.

The lowest root mean square of the weighted acceleration of $0.17\ \mathrm{m/s^2}$ is provided by the spring of 5000 N/m stiffness and shock-absorber of 750 Ns/m damping coefficient. The highest root mean square of the weighted driver's acceleration amounts to $0.31\ \mathrm{m/s^2}$ for spring stiffness of 15,000 N/m and shock-absorber damping coefficient of 400 Ns/m. Fig. 14 shows dependency of root mean square of the weighted driver's vertical acceleration as a function of the spring stiffness and the shock-absorber damping coefficient.

It is noticeable that lower root mean squares of the weighted acceleration are provided by seats with lower spring stiffness. Seats with higher spring stiffness and lower shock-absorber damping values increase root mean squares of the weighted driver's acceleration. In Fig. 14, the minimum and maximum root mean squares of the weighted driver's acceleration as well as the root mean square of the weighted acceleration for driver's seat real oscillatory parameters (see Table 6) are indicated.

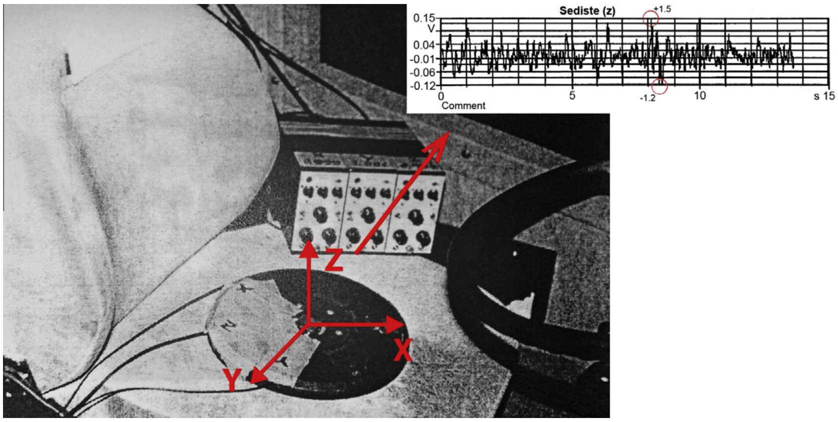

Fig. 12. Vertical acceleration on the driver's place.

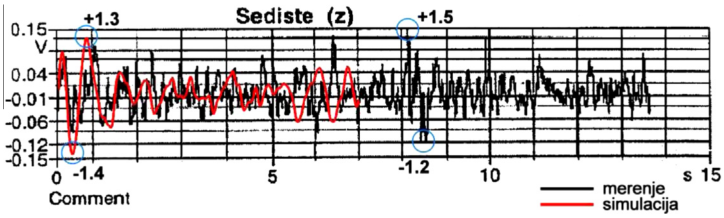

Fig. 13. Parallel representation of vertical acceleration signals established by measurements (black line) and simulation (red line). (For interpretation of the references to colour in this figure legend, the reader is referred to the web version of this article.)

Table 6
Statistical values for the driver's vertical acceleration signal established by measurements and simulation.

Statistical characteristics	Driver vertical acceleration $[m/s^2]$	
	Experimental measurements	Simulation
Minimum value	−1.20	−1.3992
Maximum value	1.50	1.2997
Mean value	0.00	−0.0006
Dispersion	0.40	0.2228

Table 7
Root mean squares of the weighted acceleration on the bus users.

Spring stiffness (N/m)	Shock-absorber damping (Ns/m)		
	400	750	1000
5000	0.2	0.17	0.18
10,000	0.28	0.23	0.22
15,000	0.31	0.26	0.24

4.2. Vibration exposure time for driver relative to the reduced comfort criterion

To determine the allowable vibration exposure time for driver relative to the reduced comfort criterion, the diagram for weighting oscillation effects in z-direction, after the 1978 ISO 2631-1 standard, was employed [14]. Root mean squares of the frequency-weighted acceleration for center frequencies of one-third octave bands were determined according to the expression

$$\ddot{z}_{rms,w}(f_i) = \sqrt{\Phi_{\ddot{z}_{rms,w}}(f_i)\triangle f_i} \tag{27}$$

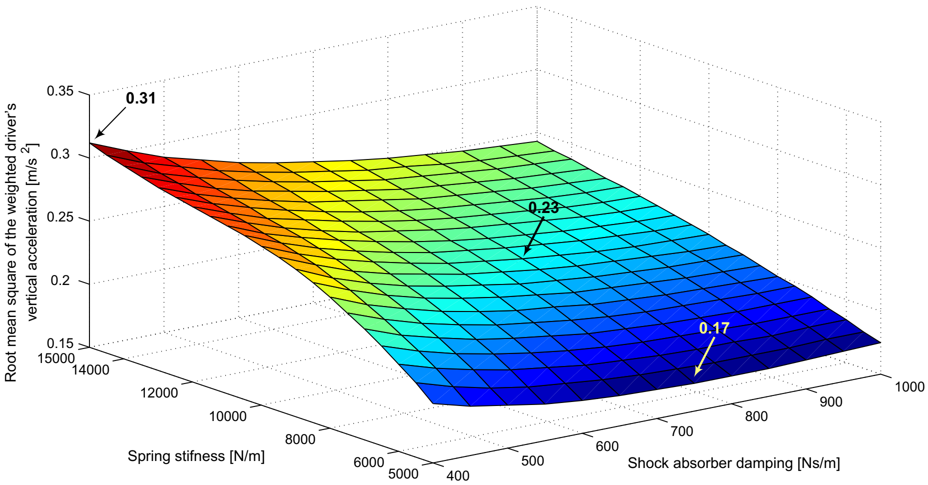

Fig. 14. Root mean square of the weighted driver's vertical acceleration as a function of the spring stiffness and shock-absorber damping coefficients of driver's seat.

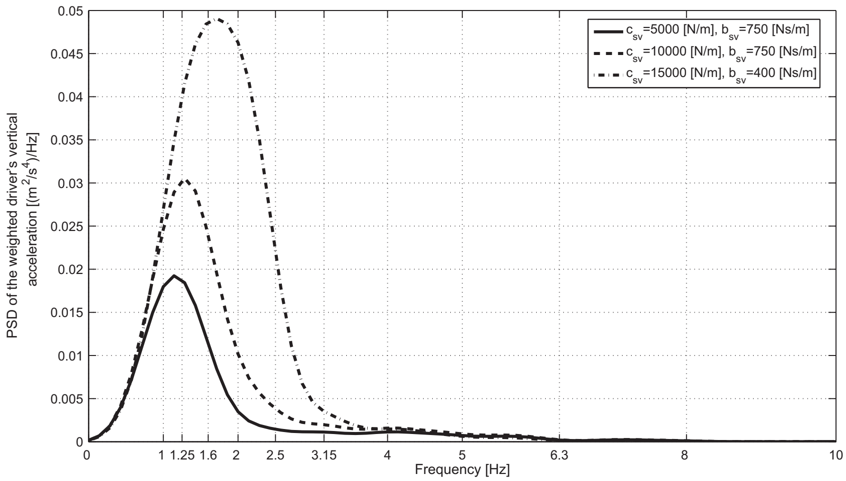

Fig. 15. PSD of the weighted driver's vertical acceleration.

where $\ddot{z}_{rms,w}(f_i)$ is the root mean square of the frequency-weighted vertical acceleration for center frequencies of one-third octave bands in $\mathrm{m/s^2}$, $\Phi_{\ddot{z}_{rms,w}}(f_i)$ is the power spectral density of weighted vertical acceleration for center frequencies of one-third octave bands in $(\mathrm{m^2/s^4})/\mathrm{Hz}$, and Δf_i is the one-third octave bandwidth for center frequencies f_i in Hz. Fig. 15 shows the power spectral densities of weighted vertical acceleration for the spring stiffness of 5000, 10,000, and 15,000 N/m and the shock-absorber damping of 400, 750, and 1000 Ns/m as a function of frequency. Power spectral densities were obtained after the Welch method which was implemented in the MATLAB Signal Processing Toolbox using the built-in function "*pwelch*()". Standard (default) values were chosen for the values of *window* and *noverlap* parameters in the above function. The length of sequence of weighted vertical acceleration of 7001 was chosen for the number of *nfft* points at which the function is computing fast Fourier transform. The frequency of signal selecting for weighted vertical acceleration of 1000 Hz was taken for the *fs* parameter value in the function "*pwelch*()".

It is noticeable that higher power spectral densities of the weighted driver's vertical acceleration correspond to the higher spring stiffness. Also, higher values of seat resonant frequencies correspond to higher spring stiffnesses. The resonant frequencies are in the frequency range of $1.0 \div 2.0$ Hz. The one-third octave bandwidths $\triangle f_i$ for the center frequencies f_i are computed according to the expression

$$\triangle f_i = f_{Ri} - f_{Li} \tag{28}$$

where f_{Li} is the lower bound frequency for center frequency f_i in Hz and f_{Ri} is the upper bound frequency for the center frequency f_i in Hz. The lower and upper bounds can be determined applying the following expressions:

Table 8
Root mean squares of the frequency-weighted acceleration for center frequencies of one-third octave bands.

f_{Li}(Hz)	f_i(Hz)	f_{Ri}(Hz)	c_{sv} = 5000 N/m b_{sv} = 750 Ns/m		c_{sv} = 10,000 N/m b_{sv} = 750 Ns/m		c_{sv} = 15,000 N/m b_{sv} = 400 Ns/m	
			$\Phi_{Zrms,w}(f_i)$	$z_{rms,w}(f_i)$	$\Phi_{Zrms,w}(f_i)$	$z_{rms,w}(f_i)$	$\Phi_{Zrms,w}(f_i)$	$z_{rms,w}(f_i)$
0.89	1	1.12	0.018	0.064	0.025	0.076	0.0275	0.08
1.1125	1.25	1.4	0.0185	0.073	0.0305	0.094	0.04	0.107
1.424	1.6	1.792	0.012	0.066	0.0245	0.095	0.049	0.134
1.78	2	2.24	0.0035	0.04	0.01	0.068	0.046	0.145
2.225	2.5	2.8	0.002	0.034	0.004	0.048	0.023	0.115
2.8035	3.15	3.528	0.0015	0.033	0.002	0.038	0.0035	0.05
3.56	4	4.48	0.0015	0.037	0.0025	0.048	0.002	0.043
4.45	5	5.6	0.001	0.034	0.001	0.034	0.0009	0.032
5.607	6.3	7.056	0.0005	0.027	0.0005	0.027	0.0005	0.027

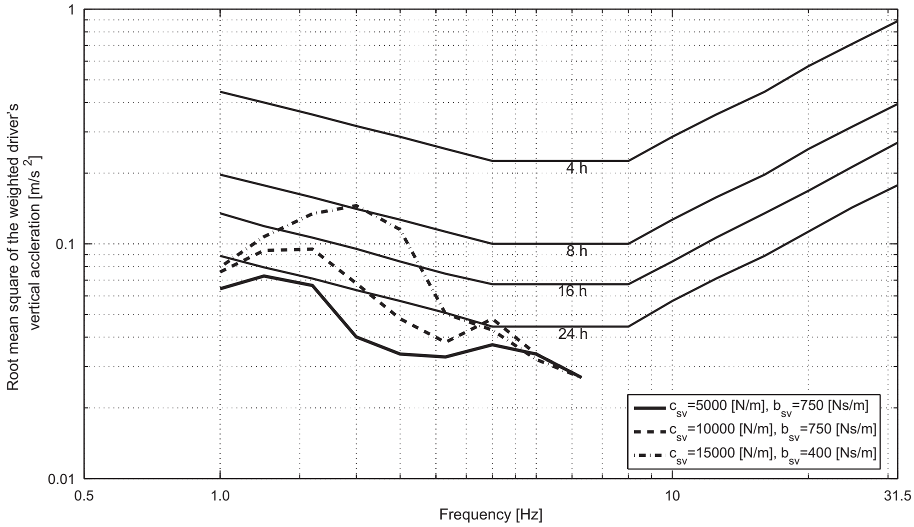

Fig. 16. Driver exposure time to oscillations in the z-axis direction for the reduced comfort criterion.

$$f_{Li} = 0.89f_i, \quad f_{Ri} = 1.26f_{Li} = 1.12f_i. \tag{29}$$

Table 8 shows the bound frequencies for the one-third octave bands, the center frequencies for the one-third octave bands, the values of power spectral densities for the center frequencies and the computed root mean squares of the frequency weighted driver's acceleration for the center frequencies.

Fig. 16 presents the 1978 ISO 2631-1 comfort curves for the vertical direction and RMS curves for the seat oscillatory parameters from Table 7. The RMS curves were obtained by integrating root mean squares of the frequency-weighted acceleration for center frequencies into the diagram. The peaks of RMS curves define the allowable driver whole-body exposure time to oscillations.

It is noticeable that the allowable driver exposure time to oscillations decreases as the driver seat spring stiffness increases. The longest allowable exposure time to oscillations, of approximately 24 h, allows for the driver's seat with the spring stiffness of 5000 N/m. The seat with the spring stiffness of 10,000 N/m allows for the exposure time longer than 16 h, while the seat with the spring stiffness of 15,000 N/m allows for the exposure time shorter than 8 h. Consequently, better oscillatory comfort for the driver requires springs of lower stiffness within the seat suspension system.

5. Conclusions

The spatial oscillatory model of the intercity bus IK-301 has been defined in the paper. The model was used to analyze the oscillatory comfort of driver and passengers on their places in the bus.

For the bus speed of 100 km/h and the asphalt-concrete excitation in a very good state, the root means square of the weighted driver's acceleration, passengers in the middle part of the bus and in the rear overhang amount to 0.23 m/s^2, 0.30 m/s^2, and 0.62 m/s^2, respectively. According to the weighting criteria from the 1997 ISO 2631-1 standard, there are vibration effects on passenger comfort in the bus rear overhang.

The driver oscillatory comfort depends on the spring stiffness and the shock-absorber damping in the driver's seat suspension system. According to the results of simulation carried out, the lowest root mean square of the weighted acceleration of $0.17\ \mathrm{m/s^2}$ is provided by the seat with the spring stiffness of 5000 N/m and the shock-absorber damping of 750 Ns/m. The highest root mean square of the weighted acceleration of $0.31\ \mathrm{m/s^2}$ was established for the seat with the highest spring stiffness of $15,000$ N/m and the lowest shock-absorber damping of 400 Ns/m. This root mean square value is close to the border value for comfort of $0.315\ \mathrm{m/s^2}$ in public means of transport, after the 1997 ISO 2631-1 standard.

The seats with the lower spring stiffness provide for the longer allowable exposure time to vibrations for the reduced comfort criterion. For the seat with the real oscillatory parameters ($c_{sv} = 10,000$ N/m, $b_{sv} = 750$ Ns/m) the allowable exposure time amounts to approximately 16 h. If the spring stiffness is reduced by 50%, the allowable exposure time is increased by approximately 50%, and vice verse. For the seats with spring stiffness of 5000 N/m and $15,000$ N/m the allowable exposure time of the driver to vibrations, according to the results of simulation carried out, amounts to, approximately, 24 h and 8 h (see Fig. 16).

The signal for the vertical driver's acceleration established by simulation for the bus real oscillatory parameters is comparable with the signal of the vertical driver's acceleration recorded in the real conditions of bus exploitation. This is indicated by peak values, statistical values, and character of change in the acceleration signal in the time domain. Apart from the vertical user's acceleration, the model defined provides for the analysis of the other oscillatory quantities. For example, the change of the vertical forces at the contacts of bus wheels and road surface, the deformations in the bus suspension system and the like.

Acknowledgements

Support for this research was provided by the Ministry of Education, Science and Technological Development of the Republic of Serbia under Grants No. TR35006 and No. TR36027. This support is gratefully acknowledged.

Appendix A. Supplementary data

Supplementary data associated with this article can be found, in the online version, at http://dx.doi.org/10.1016/j.apm.2013.03.060.

References

[1] V. Dedović, D. Mladenović, Vehicle Dynamics – Practicum, The Faculty of Transport and Traffic Engineering, Belgrade, 1999 (in Serbian).
[2] V. Dedović, Vehicle Dynamics, The Faculty of Transport and Traffic Engineering, Belgrade, 2004 (in Serbian).
[3] M.A.J. Kompier, Bus drivers: occupational stress and stress prevention, University of Nijmegen, Leiden Department of Work and Organizational Psychology, 1996.
[4] O.O. Okunribido, S.J. Shimbles, M. Magnusson, M. Pope, City bus driving and low back pain: a study of the exposures to posture demands, manual materials handling and whole-body vibration, Appl. Ergon. 38 (1) (2007) 29–38.
[5] A. Picu, Whole body vibration analysis for bus drivers, in: Proceedings of Session of the Commission of Acoustics SISOM 2009, (2009) pp. 428–431.
[6] J. Whitelegg, Health of Professional Drivers - A Report for Transport & General Workers Union, Lancaster, Eco-Logica Ltd, 1995.
[7] D. Alperovitch-Najenson, Y. Santo, Y. Masharawi, M. Katz-Leurer, D. Ushvaev, L. Kalichman, Low back pain among professional bus drivers: ergonomic and occupational-psychosocial risk factors, IMAJ 12 (2010) 26–31.
[8] C. Nelson, P. Brereton, The European vibration directive, Ind. Health 43 (2005) 472–479.
[9] G. Litak, M. Borowiec, J. Hunicz, G. KoszaÅka, A. Niewczas, Vibrations of a delivery car excited by railway track crossing, Chaos Soliton. Fract. 42 (2009) 270–276.
[10] M. Borowiec, A.K. Sen, G. Litak, J. Hunicz, G. KoszaÅka, A. Niewczas, Vibrations of a vehicle excited by real road profiles, Forsch. Ingenieurwes. 74 (2010) 99–109.
[11] R. Pečeliūnas, O. Lukoševičienė, O. Prentkovskis, A mathematical model of the vibrating system equivalent to the vehicle in the mode of emergency braking, Transport 18 (3) (2003) 136–142.
[12] R. Pečeliūnas, O. Prentkovskis, G. Garbinčius, S. Nagurnas, S. Pukalskas, Experimental research into motor vehicle oscillations in the case of changeable deceleration, Transport 20 (5) (2005) 171–175.
[13] ISO 2631: Mechanical vibration and shock-evaluation of human exposure to whole-body vibration, second ed., ISO – International Organization for Standardization, 1997.
[14] ISO 2631:Guide for the evaluation of human exposure to whole body vibration, second ed., ISO – International Organization for Standardization, 1978.
[15] Catalogue of technical data and selling prices, IKARBUS Belgrade, Factory for the production of buses and special-purpose vehicles.
[16] R. Andrzejewski, J. Awrejcewicz, Nonlinear Dynamics of a Wheeled Vehicle, Springer, New York, 2005.
[17] Q. Zhu, M. Ishitobi, Chaos and bifurcations in a nonlinear vehicle model, J. Sound Vibr. 275 (2004) 1136–1146.
[18] Q. Zhu, M. Ishitobi, Chaotic vibration of a nonlinear full-vehicle model, Int. J. Solids Struct. 43 (2006) 747–759.
[19] S. Nijemčević, D. Dragojlović, S. Zečević, B. Milosavljević et al., Technical-selling book, Beograd: Ikarbus AD, fabrika autobusa i specijalnih vozila, 2001 (in Serbian).
[20] D. Mladenović, An analysis of constructions parameters impact on the oscillatory behaviour of the bus, Master thesis, The Faculty of Transport and Traffic Engineering, Belgrade, 1997 (in Serbian).
[21] D. Simić, A. Savčić, D. Ninković, Comparative investigation of oscillatory parameters of driver's seat, MVM – Motor Veh. Engines 24–25 (1979) 7–68 (in Serbian).
[22] A. Kawamura, T. Kaku, An evaluation of road roughness and the effects on riding comfort and vehicle dynamics, Proc. of JSCE 359 (1985) 137–147.
[23] M. Shinozuka, Digital simulation of random processes and its applications, J. Sound Vib. 25 (1972) 111–128.
[24] G. Verros, S. Natsiavas, C. Papadimitriou, Design optimization of quarter-car models with passive and semi-active suspensions under random road excitation, J. Vib. Control 11 (2005) 581–606.
[25] U.V. Wagner, On non-linear stochastic dynamics of quarter car models, Int. J. Nonlinear Mech. 39 (2004) 753–765.
[26] G. Litak, M. Borowiec, M.I. Friswell, W. Przystupa, Chaotic response of a quarter car model forced by a road profile with a stochastic component, Chaos Soliton Fract. 39 (2009) 2448–2456.

[27] M.W. Sayers, Dynamic terrain inputs to predict structural integrity of ground vehicles, The University of Michigan Transportation Research Institute Ann Arbor, Michigan, 1988.
[28] Y.W. Yang, W. Cao, T.A. Chung, J. Morris, Applied Numerical Methods using Matlab, John Wiley & Sons, Inc., New Jersy, 2005.